Food Research 8 (4) : 108 - 116 (August 2024)
Journal homepage: https://www.myfoodresearch.com

FOOD RESEARCH

RESEARCH PAPER

Coomans plot classification of lard in the ink blends and ink extracts from printed packaging films using lard Fourier transform infrared spectral profile and multivariate analysis

[1,2,*]Talib, R.A., [1,2]Rashid, N.M., [1,2]Rahman, R.A., [2]Mohamad, N., [3,4]Sukor, R. and [2]Mohamad Mazlan, M.

[1] *Laboratory of Science Research, Halal Products Research Institute, Universiti Putra Malaysia, 43400 Serdang, Selangor Darul Ehsan, Malaysia*
[2]*Department of Process and Food Engineering, Faculty of Engineering, Universiti Putra Malaysia, 43400 Serdang, Selangor Darul Ehsan, Malaysia*
[3]*Department of Food Science, Faculty of Food Science and Technology, Universiti Putra Malaysia, 43400 Serdang, Selangor Darul Ehsan, Malaysia*
[4]*Institute of Tropical Agriculture and Food Security, Universiti Putra Malaysia, 43400 Serdang, Selangor Darul Ehsan, Malaysia*

Article history:
Received: 1 December 2022
Received in revised form: 1 January 2023
Accepted: 5 July 2024
Available Online: 15 July 2024

Keywords:
Lard,
Ink,
FTIR,
Partial least squares,
Discriminant analysis,
Coomans plot

DOI:
https://doi.org/10.26656/fr.2017.8(4).002

Abstract

Lard in blends of commercial gravure ink (ranging from 0.5 to 20%) and ink extracts from eleven commercially printed packaging films for foodstuffs was characterized using Fourier transform infrared (FTIR) spectroscopy. The FTIR spectral bands at 4000 – 650 cm^{-1} associated with the lard fingerprint were acquired and used to classify the lard and its blends using partial least squares (PLS) regression and discriminant analysis (DA). Commercial gravure inks (also used for preparing calibration curve samples), blends of lard ranging from 0.5 to 20% in gravure inks, and commercially printed food packaging films were tested. Linear correlation of predicted and actual values of lard were determined using PLS calibration and validation models. They produced a high coefficient of determination (R^2) of 0.943, a low root mean square error of calibration (RMSEC) of 1.674, as well as a high R^2 = 0.999 and a low root mean square error of prediction (RMSEP) of 1.233, respectively. The PLS calibration was verified employing a leave-one-out cross-validation, while DA was used to classify a series of lard standard, lard-added ink, and commercial food packaging films. The Coomans plot classification of the lard-added ink and commercial food packaging films illustrated that the food packaging samples were plotted in the right and left hemispheres in the lard-added ink class. This result also demonstrated that FTIR coupled with chemometric PLS predicted the lard content in the printing inks with high overall accuracy, as indicated by a low mean difference (MD) value of 0.577 and a low standard deviation of difference (SDD) value of 0.599. The DA allowed the ink packaging samples that potentially contained lard to be distinguished from those without lard. Sample 7 (commercially printed food packaging ink) exhibits the highest possibility of containing lard.

1. Introduction

Printing inks constitute a complex mixture of three main components, i.e., pigments (5-30%), binders or resins (5-50%), and carriers (15-80%) (Pedersen *et al*., 2012; Hu *et al*., 2018;). Moreover, additives such as oils and drying agents can contribute to as much as 10% of the formulation of the desired inks to satisfy the end-use properties (Vila and Garcia, 2012). The oils employed are mainly triglycerides, minerals, and monoesters derived from different sources, with multiple functional characteristics such as anti-blocking and anti-slip properties (Koivula *et al*., 2008). Lard or pig fat is generally more favourable for additives than other vegetable oils. It is stable over a wide temperature range and is applicable for many plastic types (Cheong and Xu, 2011; Yanty *et al*., 2014).

Additionally, lard is much cheaper; thus, adding lard or lard blended oils is common to reduce production costs (Ng *et al*., 2022). Notwithstanding the advantages of lard, as stated earlier, the presence of animal fats,

*Corresponding author.
Email: *rosnita@upm.edu.my*

eISSN: 2550-2166
Published by Rynnye Lyan Resources

particularly lard, in food, cosmetics, and pharmaceutical products, has garnered special attention and outcry from the majority of Muslim and Jewish communities due to religious restrictions. Likewise, vegetarian and vegan groups as well as health-dietary consumers will not comprehend any forms of animal fats in their consumer goods. Not limited to this range of products, halal polyolefin resin, which complies with Islamic law and is used to manufacture halal plastic products, is now commercially available for penetration of the halal market. The halal market is not only limited to the Middle East and some Southeast Asian countries, such as Malaysia and Indonesia, but also covers many countries, including China, countries in Asia, Europe, and South and North America.

Detection of lard adulteration in food systems has received much attention, and various analytical methods were previously proposed and reported. Differential scanning calorimetry (DSC), spectroscopy such as Raman and Fourier transform infrared (FTIR), chromatography including high-pressure liquid (HPLC) and gas (GC), nuclear magnetic resonance (NMR), and molecular-based methods are among those widely used for the purpose (Jaswir *et al*., 2016). Nevertheless, a limited number of studies have highlighted the rapid detection of potential adulteration in printing ink, such as the work by Ramli *et al*. (2015). This limitation is due to the difficulties in analysing the complex mixtures in these inks, which comprise organic and inorganic constituents. Nevertheless, the combination of FTIR spectra with multivariate Soft Independent Modelling of Class Analogy (SIMCA) successfully classed the samples into specific groups, namely lard, ink, calibration standard samples, and commercial ink samples. Two spectral regions i.e., full spectra (4000 – 650 cm^{-1}) and a combination of two regions (3110-2630 cm^{-1} and 1940-649 cm^{-1}), were selected to perform the Principal Component Analysis (PCA), which was employed as the basis for SIMCA. The two regions are related to the primary FTIR peaks and functional groups in lard which are observable at 3006 cm^{-1} (C=H cis), 2921 cm^{-1} (C-H asymmetrical stretch), 2852 cm^{-1} (C-H symmetrical stretch), 1749 cm^{-1} (C=O stretch), 1454 cm^{-1} (C-H bend), 1166 cm^{-1} (C-O stretch and C-H bend), and 720 cm^{-1} (CH_2 bend out) (Guntarti *et al*., 2019). In addition, a doublet peak located at 1119 cm^{-1} and 1089 cm^{-1} was apparent in lard-added ink which was associated with the overlapping of the methylene rocking and the out-of-plane bending vibration of cis-disubstituted olefins (C-H bending oleic acyl group) (Ramli *et al*., 2015).

In practice, several analytical methods are required to characterize ink constituents, such as atomic absorption spectrometry (AAS), proton-induced X-ray emission (PIXE) spectroscopy, scanning electron microscopy (SEM) coupled with energy dispersive X-ray microanalysis (EDXMA) and reflectance spectrometry (Kapoor *et al*., 2021; Manso *et al*., 2019; Villafana and Edwards, 2019). Among these methods, FTIR spectroscopy has been reported to be a rapid detection method, with an affordable price, good performance and simple procedures compared to other methods (Siddiqui *et al*., 2021). Moreover, FTIR spectroscopy is a non-destructive and fast technique for qualitative characterization and quantitative measurements (Danezis *et al*., 2016). There are several studies on the characterization of the organic and inorganic components in ink using infrared spectroscopy. Asri and coworkers (2015) combined FTIR with a chemometric technique for classifying ballpoint pen inks. Meanwhile, there has also been research that used FTIR spectroscopy to analyse the chemical composition of red pigments and inks that can be used for contemporary prints (Vila and Garcia, 2012) and to differentiate black laser toner prints used to identify counterfeiting and modification of documents (Gál *et al*., 2020).

This study aims to investigate the potential occurrence of lard in printing ink used for food packaging. This could be achieved through the unique characterization of lard using FTIR spectroscopy coupled with PLS calibration models. In the current study, the main purpose of PLS is to develop calibration models with good predictive performance and accuracy to detect lard. Furthermore, the function of multivariate analysis will be explored for the identification of the potential presence of lard in the ink of selected commercially printed food packaging films.

2. Materials and Methods

2.1 Materials

Lard was extracted from the adipose tissue of swine collected from an animal slaughterhouse in Seri Kembangan, Selangor, Malaysia following the method of Che Man *et al*. (2005) with some modification. Briefly, the adipose tissue was melted in an oven (UNB 500, Memmert GmbH+Co.KG, Schwabach, Germany) at 90-100°C for 2 hrs. The melted fat was further filtered using a muslin cloth and dried through sodium sulphate (Na_2SO_4) anhydrous before being centrifuged at 3000 rpm for 20 mins. The fat was shaken vigorously to draw off the fat layer and subjected to another centrifugation at a similar speed. Finally, the lard was re-filtered (Whatman No. 1) before being stored in a refrigerator (4°C, LY950BBC-H, SNOW, Lim Yew Marketing Sdn. Bhd., Kubang Pasu, Malaysia) under a nitrogen blanket until further analysis.

https://doi.org/10.26656/fr.2017.8(4).002

The commercial gravure ink used in the printing of laminated flexible packaging films was purchased from a local ink supplier in Seri Kembangan, Selangor. The extracts of ink were acquired from the de-inking of eleven different commercially printed packaging films for foodstuffs purchased from a local retail market. For each packaging film, several pieces of 2 × 2 cm square-cut films were obtained from the printed area. The square films were soaked separately in a beaker containing sodium hydroxide (NaOH) and zirconium beads (acting as an abrasive agent) before stirring until the ink detached from the film in a hot water bath at 60°C for 8 hrs. The detached ink mixture was centrifuged for 5 mins at 6000 rpm. The supernatant in the individual mixture was discarded, and the precipitate containing the detached ink was oven-dried at 40°C before the sample was ready for FTIR spectral acquisition.

2.2 Quantitative analysis method

The quantitative analysis of lard in inks was carried out using the partial least square (PLS) method. In establishing the PLS model, standard samples for the calibration set were acquired by spiking a series of lard concentrations ranging from 0.5-20% into commercial gravure ink. All the lards were weighed at different amounts to facilitate the calculation of the actual percentage of added lard in the gravure ink formulation. A Nicolet 6700 FTIR spectrometer (Thermo Electron Corp., USA) was used to acquire the spectra of the blends. For validation, nine independent samples were constructed, which included various concentrations of lard within the set range.

2.3 Discriminant Analysis

A series of lab-produced lards (with compositions ranging from 50-100% designated lard), lard-added ink and commercial food packaging film samples were used in the discriminant analysis by using TQ Analyst™ version 6 software (Thermo Electron Corp., USA). In the first part of the study, a standard series of pure lard (100%) and lard-added ink were compared and classified, followed by lard-added ink and commercially printed packaging samples.

2.4 FTIR Analysis

Different concentrations of commercial-grade ink and lard blends of the ink were scanned using a Nicolet 6700 FTIR spectrometer (Thermo Nicolet Corp, USA), equipped with a set of deuterated triglycine (DTGS) detectors through their spectral bands. The spectrometer was equipped with a KBr/germanium beam splitter that operated using an OMNIC operating system (Version 7.0 Thermo Nicolet) software. The FTIR data of 32 scans were analysed in the 4000 – 650 cm^{-1} frequency regions at a resolution of 4 cm^{-1}. These spectra were normalised by subtracting the background air spectrum. Using similar equipment attached to a conserved desiccated interferometer, the printed packaging samples (film form) were characterized. Single reflection ATR analysis was done using a smart OMNI-sampler with a sampling surface of a 2 mm diameter and a 45° crystal angle, producing a 0.67 µm infrared beam, recorded as absorbance.

2.5 Statistical analysis

The TQ Analyst™ version 6 software (Thermo Electron Corp, USA) was employed for acquiring the PLS calibration and validation models as well as for classifying the range of lard compositions added to the commercial inks. The calibration and validation model performances were analysed for a high quality of fit using the high coefficient value of determination R^2 (R^2 > 0.9-1) and a low root mean square error of calibration (RMSEC). The predictive ability of the PLS method was assessed by computing the final RMSEP and R^2 values. The PLS method was further validated using the mean difference (MD) and standard deviation of difference (SDD) to obtain high reproducibility and accuracy.

3. Results and discussion

3.1 Characterization of lard

Figure 1 illustrates the mid-region of the lard FTIR spectrum (4000 – 650 cm^{-1}). The functional groups, degree of unsaturation, length, and composition of lard can be determined by the peaks and shoulders of the spectrum (Kurniawati *et al*., 2014). The significant group frequencies of the lard are saturated and monounsaturated triglycerides (Azir *et al*., 2017). The small band of the lard spectrum at 3471 cm^{-1} within the spectral region of 3500-3280 cm^{-1} results from the overtone absorption of glyceride ester carbonyl

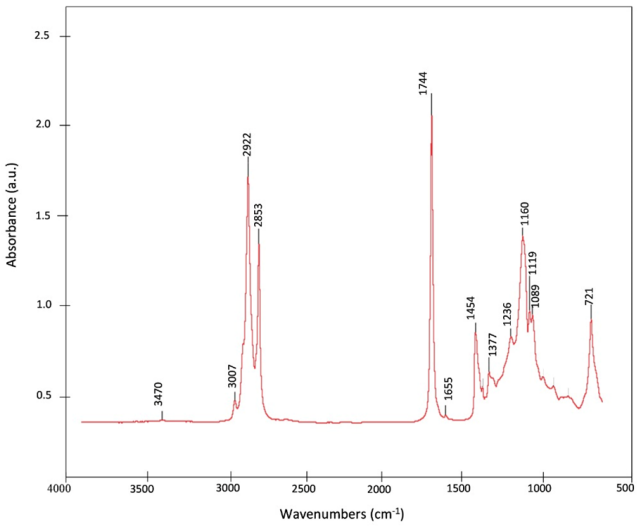

Figure 1. Mid-region of lard FTIR spectrum.

https://doi.org/10.26656/fr.2017.8(4).002

(Georgieva *et al*., 2013). In contrast, within the spectral region of 3250 to 2800 cm^{-1}, the high-frequency side of the peak at 2922 cm^{-1} corresponds to the stretching vibration of =C-H (trans). Furthermore, the small peak at 3007 cm^{-1}, which is produced by *cis* olefinic double bonds, is almost exclusively indicative of unsaturation (Chiplunkar and Pratap, 2016). The presence of methylene asymmetrical stretching appears at 2922 cm^{-1}; additionally, methylene symmetrical stretching bands appear at 2853 cm^{-1}.

In the region of 1800-1600 cm^{-1}, there is a peak at 1744 cm^{-1}, indicating C=O from the ester group. According to Yang and Irudayaraj (2000), the small band at 1655 cm^{-1} relates to the C=C stretching vibration of the disubstituted *cis* C=C of the acyl groups in the oleic and linoleic acids in the fat. The appearance of peaks between 1500 cm^{-1} and 1300 cm^{-1} shows that the scissoring band at 1454 cm^{-1} corresponds to the methylene group bending vibration. In contrast, the band at 1418 cm^{-1} is attributed to the CH bonds of *cis*-disubstituted olefin rocking vibrations. The peaks at 1377 cm^{-1} are a result of methyl group symmetrical bending vibration. According to Coates (2000), the strong methylene and methyl band at 1470 cm^{-1}, the weak methyl band at 1380 $cm^{-1,}$ and the methylene rocking vibration at 725-720 cm^{-1} indicate a long chain linear aliphatic structure.

The following bands can be observed in the region of 1300-1000 cm^{-1}. The bands at 1236 cm^{-1}, 1160 cm^{-1}, 1119 cm^{-1}, 1089 cm^{-1}, and 1032 cm^{-1} can be attributed to the stretching vibration of the C-O group in ester. Syahariza *et al*. (2005) reported the presence of doublet peaks at 1117 cm^{-1} and 1097 cm^{-1} attributed to saturated acyl groups and oleic acyl groups, respectively. This major characteristic peak of lard results from the high proportion of monounsaturated acyl groups in oleic acid (C18:1) (Fasciotti *et al*., 2020). Between the 1000-700 cm^{-1} region, the small band observed at 965 cm^{-1} corresponds to the out-of-plane bending vibration of *trans* disubstituted olefinic groups. In addition, the 721 cm^{-1} band might be attributed to the out-of-plane bending vibration of *cis*-disubstituted olefins and to overlapping methylene rocking vibration.

3.2 Characterization of lard-added Ink

A comparison between the FTIR spectra of gravure ink and 2% lard-added ink (4000 – 650 cm^{-1}) is illustrated in Figure 2. Peaks at approximately 3470 cm^{-1}, which are indicative of hydroxyl (O-H) groups, and 3150 -3000 cm^{-1} result from =C-H (trans) and =C-H (cis) groups, represented by two-small and medium peaks were exhibited by both gravure and 2% lard-added ink. Additionally, the alkane group is detected in both inks due to the asymmetrical and symmetrical stretches of the C-H bond at 2920 cm^{-1} and 2853 cm^{-1}. Stretching of C=O was represented at 1744 cm^{-1}, whereas the vibration of $N\text{-}H_1$ amines was seen at 1647 cm^{-1} and 1539 cm^{-1}. Furthermore, bending of C-H, symmetrical bending of C -H (CH_3), and -C-H (CH_3) bending were attributed to 1454 cm^{-1} and 1377 cm^{-1}, respectively. The C-O stretching vibration in the ester resulted in vibrational peaks at 1240 cm^{-1}, 1119 cm^{-1}, and 1089 cm^{-1}. Other peaks at 947 cm^{-1}, 886 cm^{-1}, 812 cm^{-1}, and 715 cm^{-1} corresponded to $N\text{-}H_{1,2}$ amines and C-H bending.

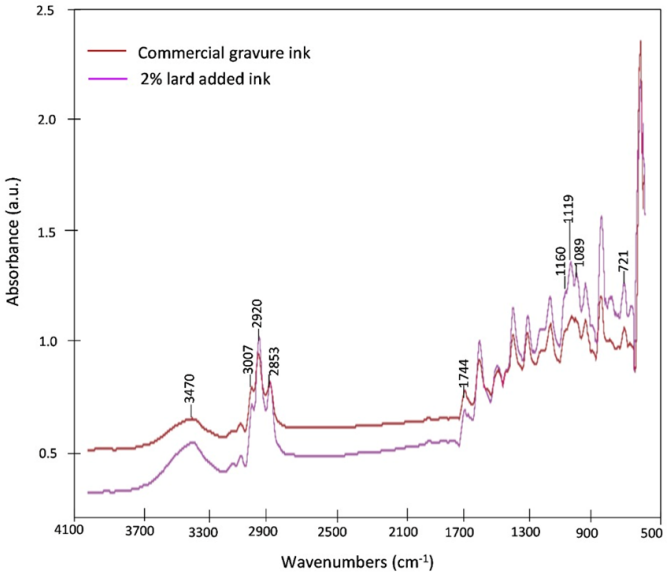

Figure 2. Comparison between FTIR spectra of commercial gravure ink and 2% lard-added ink. The labelled peaks indicate significant absorption bands in the determination of lard.

The differences between gravure ink and the 2% lard-ink spectrum can be seen from an apparent doublet peak 1119 cm^{-1} and 1089 cm^{-1} that is only present in the 2% lard-ink spectrum. The shoulder peak at a lower wavenumber of 1089 cm^{-1} of the doublet peak is detected as absent in the gravure ink spectrum. This can be due to the overlapping of the methylene rocking (saturated acyl group) and the out-of-plane bending vibration of cis-disubstituted olefins (C-H bending oleic acyl group). Ramli *et al*. (2015) reported that the peak at 1089 cm^{-1} was identified as one of the major characteristic peaks in lard due to the high proportion of monounsaturated acyl group of oleic acid. In addition, the peak at 721 cm^{-1} was observed as the most intense peak feature in the 2% lard-ink spectrum while detected as absent in the gravure ink spectrum. This peak which corresponds to methylene rocking vibration indicate a long chain linear aliphatic structure. Thus, it can be concluded that these characteristic peaks refer exclusively to lard in the 2% lard-added ink spectrum. Furthermore, increasing the carboxyl (C=O) absorption by adding 2% lard to gravure ink corresponded to increases in the peak intensity at

https://doi.org/10.26656/fr.2017.8(4).002

approximately 1744 cm^{-1}. A similar peak value was observed by Guillen and Cabo (1998) and Bahri and Che Man (2016) which was associated with the C=O group of triglyceride ester linkage. Table 1 lists the peak intensities of gravure ink and 2% lard-added ink from selected frequency regions. It can be observed that the peaks including 1119 cm^{-1}, 1377 cm^{-1}, 1454 cm^{-1}, 1733 cm^{-1}, 1744 cm^{-1}, 2853 cm^{-1}, 2920 cm^{-1}, and 3023 cm^{-1} are considerably more intense in the 2% lard-ink than the gravure ink spectrum. This implies that the peak from both inks overlap leading to higher intensity. Table 2 represents the characteristic infrared absorption peaks of lard and gravure ink. For comparison between gravure ink and lard-added ink spectra, the lowest range value 2% lard loading was selected to exhibit that lard content as low as 2% in the ink mixture could be detected with good accuracy of prediction using the FTIR spectra combining with multivariate analysis. Other authors have reported that as low as 5% of lard in the printing ink was detected using FTIR spectroscopy (Ramli *et al*., 2015).

Table 1. Peak intensity values of gravure ink and 2% lard-added gravure ink from selected frequency regions.

Wavenumbers (cm^{-1})	Absorbance	
	Gravure ink	2% lard-added gravure ink
721	0.000	4.371
1089	0.000	2.354
1119	2.185	2.435
1377	2.016	2.056
1454	2.001	2.109
1744	1.359	1.393
2853	1.492	1.595
2920	1.806	1.903
3023	1.160	1.175

3.3 Characterization of commercial printed packaging films

FTIR spectra of the eleven commercial printed packaging films acquired via the ATR tower mode are presented in Figure 3. Absorption peaks at 721 cm^{-1}, 1089 cm^{-1} and 1119 cm^{-1} correspond to the significant primer characteristics of lard in the determination. Small peaks were observed at regions of 3000-2800 cm^{-1}, 1800 -1700 $cm^{-1,}$ and 1300-600 cm^{-1}, indicating features of oil. According to Pan and Nguyen (2007), the peaks at 2925 cm^{-1}, 2855 cm^{-1}, 1460 cm^{-1}, 1375 cm^{-1}, 1237 cm^{-1}, 1160 cm^{-1}, 1098 cm^{-1}, 914 cm^{-1}, and 720 cm^{-1} correspond to acrylic ($-CH_2$) or C-H stretching of alkanes, whereas the peak at 1744 cm^{-1} corresponds to the C=O stretching of a carbonyl group. Different concentrations of O-H were represented by peaks at 3200-3700 cm^{-1} range and the peak at 1384 cm^{-1} was due to C-H deformation. Meanwhile, for the amine group, N-H_1 and N-$H_{1,2}$ amines were represented by 1627 cm^{-1} and 1559 cm^{-1} for N-H_1 and 620 cm^{-1} for N-$H_{1,2}$, respectively. These amine groups correspond to amines and ammonia, which act as the main components in water-based ink that regulate stability and efficiency, according to Li *et al*. (2020).

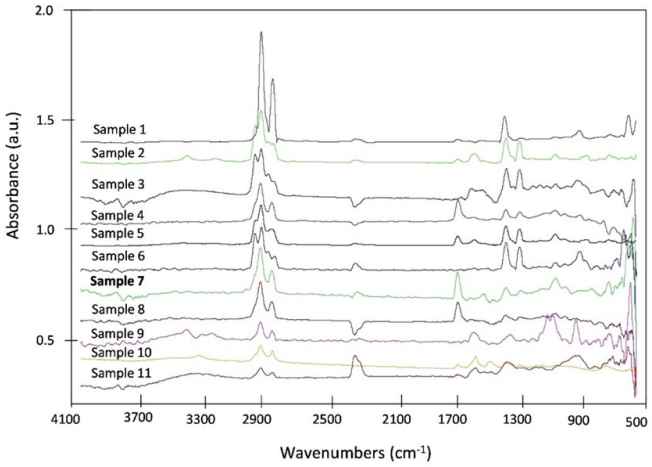

Figure 3. FTIR spectra of eleven commercially printed food packaging films.

Moreover, the typical peak frequencies from the polyethylene film also overlap with the peaks from the ink spectrum. Bumbudsanpharoke *et al*. (2022) reported that a major characteristic of polyethylene is a strong doublet vibrational mode at approximately 1471 cm^{-1}. In addition, the vibration at approximately 1462 cm^{-1} is

Table 2. Characteristics of infrared absorption peaks of lard and gravure ink.

Sample	Wavenumbers (cm^{-1})	Functional Group Assignment
Lard	721	Overlapping C-H rocking vibration and out-of-plane vibration of cis-disubstituted olefins
	1089	C-H bending in oleic acyl groups
	1119	Saturated acyl groups
	1377	Symmetric bending vibration of CH_3 group
	1454	Bending vibrations of CH_2 and CH_3 aliphatic group
	1744	Ester saturated aliphatic (C=O)
	2850-2980	Symmetric and asymmetric C-H stretching of methyl and methylene groups
	3007	Unsaturation (C=C-H)
Gravure Ink	700-610	–C≡C-H: C–H alkynes
	1200-1000	C-O stretching, asymmetric stretching
	1721	Carbonyl groups (C=O)
	2920, 2853	Symmetric and asymmetric C-H stretching of methyl and methylene groups
	3575-3125	Hydroxyl (O-H) groups

https://doi.org/10.26656/fr.2017.8(4).002

assigned as a C-H bending motion. Moreover, the doublet vibrations at approximately 730 cm^{-1} and 720 cm^{-1} correspond to the C-H rocking motion. These features can be observed in all the samples in the current study but with small peak intensities. Table 3 summarizes the peak assignments of commercially printed packaging films at selected frequency regions of peak 721 cm^{-1} and doublet peak 1089 cm^{-1} and 1119 cm^{-1}. The result suggested that sample 7 has the highest possibility of containing lard, displaying the presence of the peak in all the selected frequencies. On the other hand, sample 10 is improbable to contain lard due to no absorption peaks at 1089 cm^{-1} and 1119 cm^{-1}. Samples 4 and 6 were also considered not to contain lard due to the absence of peak 1119 cm^{-1}.

Table 3. Peak assignments of commercial printed food packaging films in selected frequency region.

Sample	Wavenumbers (cm^{-1})		
	721	1089	1119
1	/	-	-
2	-	-	-
3	/	-	/
4	/	/	-
5	/	-	-
6	/	/	-
7	/	/	/
8	/	-	-
9	/	-	/
10	/	-	-
11	/	-	/

(/) = present; (-) = not present

3.4 Partial least square calibration and cross-validation

The calibration and validation models were developed using PLS statistical techniques to predict the FTIR spectra and the actual data using the non-baseline type in the spectral region of 4000 – 650 cm^{-1}. Figure 4 presents a plot of the actual value for samples containing different percentages of blended lard (%v/v) in the ink formulation against the FTIR predicted value. The best linear regression model, y = 0.989x + 0.570, was obtained from the graph. This is indicated by the high value of the coefficient of determination (R^2 = 0.943) and the low value of the root mean square error of calibration (RMSEC = 1.674), presenting a high reliability of the regression model.

Figure 5 illustrates the PLS cross-validation linear regression model for the relationship between the actual value of lard in the lard-added ink and the FTIR predicted value. The best regression model of y = 0.973x + 1.113 was yielded, as indicated by a high R^2 value of 0.999. The final R^2 value of 0.999 and the RMSEP value of 1.233 were obtained after removing one standard at a time. In addition, low MD (0.577) and SDD (0.599) values were obtained, indicating that the PLS-FTIR models have high performance predicting the lard present. Overall, the statistical values demonstrated that FTIR, coupled with multivariate analysis, is an accurate method for quantitative analysis.

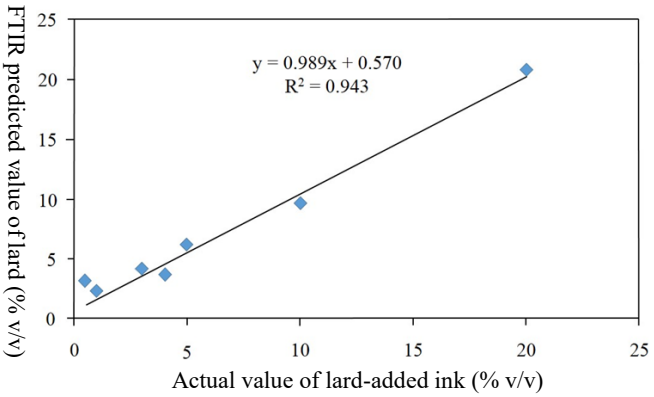

Figure 4. Calibration curve of the actual value of lard-added ink versus FTIR predicted value of lard.

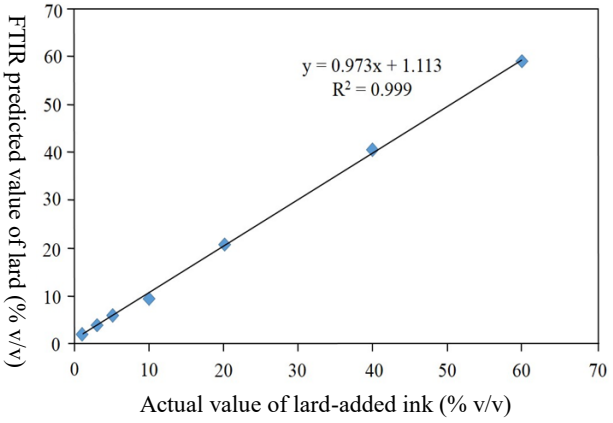

Figure 5. PLS cross-validation graph of FTIR actual value of lard-added ink versus FTIR predicted value of lard by leave-one-out cross-validation.

3.5 Discriminant analysis

Class membership of simultaneous observations between two models can be discriminated using the Coomans plot. A small distance between the models implies that the classification model is insufficient to separate the classes from each other. The analysis used the Mahalanobis distance to differentiate the resemblance between an unknown sample and the known measured samples. The perpendicular grey lines of the boundaries between the x- and y-axes represent 95% confidence intervals. From the Coomans plot, the standard for the y-axis is well-defined if the data points cluster whereas the standards of the x-axis are well-defined data points clustered in the lower right corner of the plot. Moreover, if the data points fall inside the boundary (grey line) for the selected class, the two classes are similar.

Figure 6 demonstrates the classification of Coomans plot of lard and lard-added ink in the 4000 – 650 cm^{-1}

https://doi.org/10.26656/fr.2017.8(4).002

frequency range. The figure shows the distance for the lard versus the distance for the lard-added ink. It is noted that the two groups are separated well and located at their respective axes. According to Manaf and coworkers (2007), some samples may be misclassified since the chemical composition are too close to one another. However, one sample of lard-added ink is classified as an outlier or not belonging to any classes.

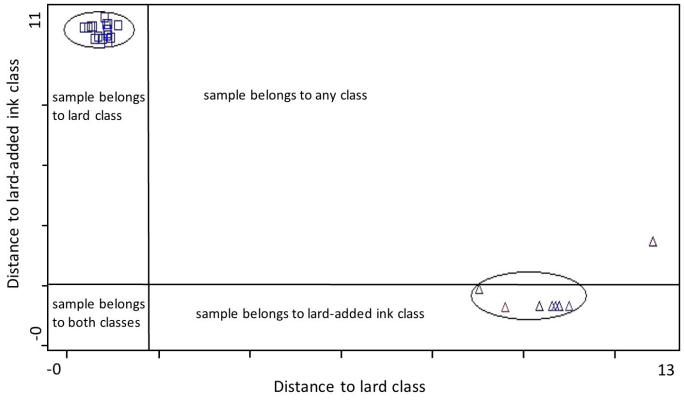

Figure 6. The Coomans plot of (□) lard versus (Δ) lard-added ink.

Figure 7 graphically shows the Coomans plot classification of the lard-added ink and the commercially printed package samples in the 4000 – 650 cm^{-1} frequency range. Mahalanobis distance for the lard-added ink and the distance for the commercially printed packages are represented by x-axis and y-axis, respectively. It is noteworthy that the data points are classified into two groups well. One data point of the printed package sample exhibits the closest distance to the lard-added ink model, whereas three samples are plotted longer distances to the right side. Additionally, the group of seven samples is plotted further in the right hemispheres, indicating longer distances from the lard-added ink model. Thus, a shorter distance from the ink-added class indicates that the samples have a high potential of containing lard in their printing ink formulations or that they might be similar in their chemical compositions.

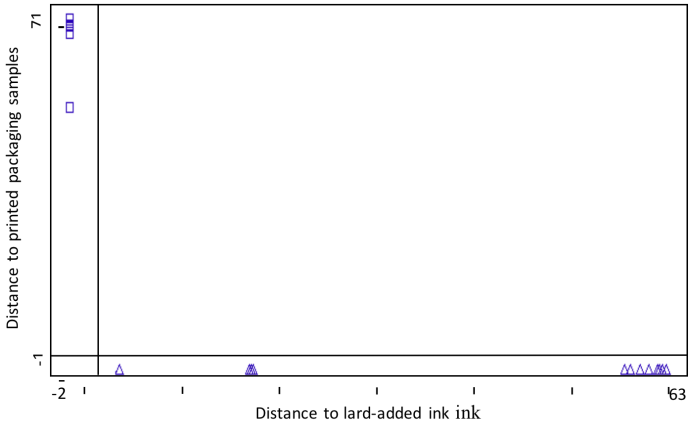

Figure 7. The Coomans plot of (□) lard-added ink versus (Δ) commercially printed food packaging films.

4. Conclusion

A combination of FTIR spectroscopy with partial least square (PLS) regression and discriminant analysis (DA) was able to determine the presence of lard in lard-added commercial gravure ink (0.5 – 20% of lard) and commercial printed food packaging films. FTIR spectroscopy revealed that gravure ink containing 2% lard has greater peak intensity values than gravure ink containing 0% lard, as determined from certain frequency ranges. The majority of the commercial printed food packaging samples examined showed a peak in the 720 – 725 cm^{-1} regions, corresponding to C-H rocking motion. The PLS calibration linear curve (R^2 = 0.943) and PLS cross-validation linear curve (R^2 = 0.999) of FTIR prediction value of lard (% v/v) for the lard-added commercial gravure ink was successfully developed. Coomans plot with Mahalanobis distance in DA successfully sorted all samples into two groups. In the 4000 – 650 cm^{-1} frequency range, lard-added commercial gravure ink and commercial printed food packaging samples were categorized as lard and lard-added gravure ink classes. The classification of commercial printed food packaging samples showed that sample 7 exhibits the closest distance to the lard-added gravure ink class. In contrast, the others lie at a longer distance. In conclusion, the commercial printed food packaging closer to the lard-added ink class suggests that the sample has a high possibility of incorporating lard in their printing formulations or that they may have comparable chemical compositions.

Conflict of interest

The authors declare no conflicts of interest.

Acknowledgements

This research was supported by the Ministry of Higher Education of Malaysia (MOHE) through the Fundamental Research Grant Scheme (FRGS/2/2013/SG01/UPM/02/4). We also intend to thank Universiti Putra Malaysia (UPM) for granting Graduate Research Fellowship (GRF) to Norma M. Rashid and Halal Products Research Institute (UPM) for allowing us to use all research facilities.

References

Asri, M.N.M., Mat Desa, W.N.S. and Wan Dzulkiflee, I. (2015). Fourier transform infrared (FTIR) spectroscopy with chemometric techniques for the classification of ballpoint pen inks. *Arab Journal of Forensic Sciences and Forensic Medicine*, 1(2), 194-200.

Azir, M., Abbasiliasi, S., Tengku Ibrahim, T.A., Manaf,

Y.N.A., Sazili, A.Q. and Mustafa, S. (2017). Detection of lard in cocoa butter—its fatty acid composition, triacylglycerol profiles, and thermal characteristics. *Foods*, 6(11), 98. https://doi.org/10.3390/foods6110098

Bahri, S.S. and Che Man, Y.B. (2016). Rapid detection of lard in chocolate and chocolate-based food products using Fourier transform infrared spectroscopy. *Journal of Tropical Agriculture and Food Science,* 44(2), 253-263.

Bumbudsanpharoke, N., Wongphan, P., Promhuad, K., Leelaphiwat, P. and Harnkarnsujarit, N. (2022). Morphology and permeability of bio-based poly (butylene adipate-co-terephthalate) (PBAT), poly (butylene succinate) (PBS) and linear low-density polyethylene (LLDPE) blend films control shelf-life of packaged bread. *Food Control*, 132(18), 108541. https://doi.org/10.1016/j.foodcont.2021.108541

Che Man, Y.B., Syahariza, Z.A., Mirghani, M.E.S., Jinap, S. and Bakar, J. (2005). Analysis of potential lard adulteration in chocolate and chocolate products using Fourier transform infrared spectroscopy. *Food Chemistry*, 90(4), 815-819. https://doi.org/10.1016/j.foodchem.2004.05.029

Cheong, L.Z. and Xu, X. (2011). Lard-based fats healthier than lard: Enzymatic synthesis, physicochemical properties and applications. *Lipid Technology*, 23(1), 6-9. https://doi.org/10.1002/lite.201100077

Chiplunkar, P.P. and Pratap, A.P. (2016). Utilization of sunflower acid oil for synthesis of alkyd resin. *Progress in Organic Coatings*, 93, 61-67. https://doi.org/10.1016/j.porgcoat.2016.01.002

Coates, J. (2000). Interpretation of Infrared Spectroscopy, A Practical Approach. In Meyers, R.A. (Ed). Encyclopedia of Analytical Chemistry, p. 10815-10837. Chichester, UK: John Wiley and Sons Ltd.

Danezis, G.P., Tsagkaris, A.S., Camin, F., Brusic, V. and Georgiou, C.A. (2016). Food authentication: Techniques, trends and emerging approaches. *Trends in Analytical Chemistry*, 85(Part A), 123-132. https://doi.org/10.1016/j.trac.2016.02.026

Fasciotti, M., Monteiro, T.V., Rocha, W.F., Morais, L.R., Sussulini, A., Eberlin, M.N. and Cunha, V.S. (2020). Comprehensive triacylglycerol characterization of oils and butters of 15 amazonian oleaginous species by ESI-HRMS/MS and comparison with common edible oils and fats. *European Journal of Lipid Science and Technology*, 122(9), 2000019. https://doi.org/10.1002/ejlt.202000019

Gál, L., Oravec, M., Kiššová, M., Gemeiner, P. and Čeppan, M. (2020). Forensic discrimination of black laser prints by a combination of chemometric methods and μ-ATR-FTIR spectroscopy. *Chemical Papers*, 74(10), 3269-3277. https://doi.org/10.1007/s11696-020-01145-x

Georgieva, K., Petkov, P. and Denev, Y. (2013). Study and classification of vegetable oils using the Fourier transform infrared spectroscopy. *Oxidation Communications*, 36(1), 85-93.

Guillen, M.D. and Cabo, N. (1998). Relationships between the composition of edible oils and lard and the ratio of the absorbance of specific bands of their Fourier transform infrared spectra. Role of some bands of the fingerprint region. *Journal of Agriculture and Food Chemistry,* 46(5), 1788-1793. https://doi.org/10.1021/jf9705274

Guntarti, A., Ahda, M., Kusbandari, A. and Prihandoko, S.W. (2019). Analysis of lard in sausage using Fourier transform infrared spectrophotometer combined with chemometrics. *Journal of Pharmacy and Bioallied Sciences*, 11(Suppl. 4), S594. https://doi.org/10.4103/jpbs.JPBS_209_19

Hu, G., Kang, J., Ng, L.W., Zhu, X., Howe, R. C., Jones, C. G., Hersam, M.C. and Hasan, T. (2018). Functional inks and printing of two-dimensional materials. *Chemical Society Reviews*, 47(9), 3265-3300. https://doi.org/10.1039/C8CS00084K

Jaswir, I., Mirghani, M.E.S., Salleh, H.M., Ramli, N., Octavianti, F. and Hendri, R. (2016). An overview of the current analytical methods for halal testing. In Ab. Manan S., Abd Rahman F., Sahri M. (Eds). Contemporary Issues and Development in the Global Halal Industry, p. 291-298. Singapore: Springer. https://doi.org/10.1007/978-981-10-1452-9_27

Kapoor, N., Sulke, P., Shukla, R.K., Kakad, R., Pardeshi, P. and Badiye, A. (2021). Forensic analytical approaches to the dating of documents: An overview. *Microchemical Journal*, 170, 106722. https://doi.org/10.1016/j.microc.2021.106722

Koivula, H., Preston, J.S., Heard, P.J. and Toivakka, M. (2008). Visualization of the distribution of offset ink components printed onto coated paper. *Colloids and Surface A: Physicochemical and Engineering Aspects,* 317(1-3), 557-567. https://doi.org/10.1016/j.colsurfa.2007.11.043

Kurniawati, E., Rohman, A. and Triyana, K. (2014). Analysis of lard in meatball broth using Fourier transform infrared (FTIR) spectroscopy and chemometrics. *Meat Science,* 96(1), 94-98. https://doi.org/10.1016/j.meatsci.2013.07.003

Manaf, M.A., Che Man, Y.B., Hamid, N.S.A., Ismail, A.

and Syahariza, Z.A. (2007). Analysis of adulteration of virgin coconut oil by palm kernel olein using Fourier transform infrared spectroscopy. *Journal of Food Lipid*s, 14(2), 111-121. https://doi.org/10.1111/j.1745-4522.2007.00066.x

Manso, M., Pessanha, S., Guerra, M., Reinholz, U., Afonso, C., Radtke, M., Lourenço, H., Carvalho, M.L. and Buzanich, A.G. (2019). Assessment of toxic metals and hazardous substances in tattoo inks using Sy-XRF, AAS, and Raman spectroscopy. *Biological Trace Element Research*, 187(2), 596-601. https://doi.org/10.1007/s12011-018-1406-y

Ng, P.C., Ahmad Ruslan, N. A. S., Chin, L.X., Ahmad, M., Abu Hanifah, S., Abdullah, Z. and Khor, S.M. (2022). Recent advances in halal food authentication: Challenges and strategies. *Journal of Food Science*, 87(1), 8-35. https://doi.org/10.1111/1750-3841.15998

Pan, J. and Nguyen, K.L. (2007). Development of the photoacoustic rapid-scan FT-IR-based method for measurement of ink concentration on printed paper. *Analytical Chemistry*, 79(6), 2259-2265. https://doi.org/10.1021/ac061732y

Pedersen, G.A., Carlson, E., Ekroth, S., Kostamo, P., Nordström, Å.L, Olafsson, G., Rajakangas, L., Vaz, R. and Fabech, B. (2012). Food contact materials and articles, printing inks: Checklists for compliance in industry and trade and control by food inspection, p. 13-14. København, Denmark: Nordic Council of Ministers.

Ramli, S., Talib, R.A., Rahman, R.A., Zainuddin, N., Othman, S.H. and Rashid, N.M. (2015). Detection of lard in ink extracted from printed food packaging using Fourier transform infrared spectroscopy and multivariate analysis. *Journal of Spectroscopy,* 2015, 502340. https://doi.org/10.1155/2015/502340

Siddiqui, M.A., Khir, M.H.M., Witjaksono, G., Ghumman, A.S.M., Junaid, M., Magsi, S.A. and Saboor, A. (2021). Multivariate analysis coupled with M-SVM classification for lard adulteration detection in meat mixtures of beef, lamb, and chicken using FTIR spectroscopy. *Foods*, 10(10), 2405. https://doi.org/10.3390/foods10102405

Syahariza, Z.A., Man, Y.B.C., Selamat, J. and Bakar, J. (2005). Detection of lard adulteration in cake formulation by Fourier transform infrared (FTIR) spectroscopy. *Food Chemistry*, 92(2), 365-371. https://doi.org/10.1016/j.foodchem.2004.10.039

Vila, A. and Garcia, J.F. (2012). Analysis of the chemical composition of red pigments and inks for the characterization and differentiation of contemporary prints. *Analytical Letters,* 45(10), 1274-1285. https://doi.org/10.1080/00032719.2012.673100

Villafana, T. and Edwards, G. (2019). Creation and reference characterization of Edo period Japanese woodblock printing ink colorant samples using multimodal imaging and reflectance spectroscopy. *Heritage Science*, 7, 94. https://doi.org/10.1186/s40494-019-0330-6

Yang, H. and Irudayaraj, J. (2000). Characterization of semisolid fats and edible oils by Fourier transform infrared photoacoustic spectroscopy. *Journal of the American Oil Chemists' Society*, 77, 291-295. https://doi.org/10.1007/s11746-000-0048-y

Yanty, N.A.M., Marikkar, J.M.N. and Abdulkarim, S. (2014). Determination of types of fat ingredient in some commercial biscuit formulations. *International Food Research Journal,* 21(1), 277-282.

https://doi.org/10.26656/fr.2017.8(4).002